Supporting Materials

Towards an industrial perspective for urea-to-hydrogen valorization by electro-oxidation on nickel(III): real effluents and pilot-scale proof of concept

Guillaume Hopsort*[,1], Elyes Piguet[1], Laure Latapie[1], Karine Groenen Serrano[1], Karine Loubière[1], Théodore Tzedakis*[,1]

Correspondence: hopsort.guillaume@gmail.com and theodore.tzedakis@univ-tlse3.fr

Laboratoire de Génie Chimique, Université de Toulouse, CNRS, INPT, UPS, Toulouse, France

Table of contents

1 Experimental

1.1 Chemicals

All the chemicals used in this work were provided by Sigma-Aldrich (USA). Ultra-pure water (18 MΩ.cm) was used to prepare the alkalinized solutions with a KOH concentration of 1 mol.L^{-1}, leading to pH = 14. Human urine samples were collected from two healthy male participants between the ages of 25 and 30 years. Urine sample was stored at 4 °C between experiments. Repeatability was ensured by duplicating the assays using the same batch of urine.

1.2 EC set-up at lab-scale

The EC experiments were conducted as already presented in our previous work [1] utilizing a PGSTAT 128 N potentiostat from Metrohm Autolab®, managed by NOVA software. A $Hg/HgO/OH^-$ reference electrode from Origasens, Origalys® housed in a Luggin capillary filled with a supporting electrolyte of 1 mol.L^{-1} KOH was used. The potentials were systematically expressed with respect to Hg/HgO, with $E^{\circ}_{Hg/HgO}$ equal to 107 mV *vs.* SCE (for NaOH at 1 mol L^{-1}). For this study, a standard three-electrode thermally controlled cell was used. Each voltammogram was taken three times. The total electrolyte content was 50 mL. The nickel rotating disk electrode with an area of 3.14 mm^2, encased in a Teflon shaft, served as the working electrode. Conversely, the counter electrode was made up of a 316L stainless plate.

1.3 EC set-up at pilot-scale

A pilot-scale EC reactor and its surrounding environment was specially designed and built for this work. It consisted of a tubular-geometry reactor (⌀ 52 mm, 300 mm high) which features include:

- *(i)* a central tubular cathode (⌀ 10 mm), fabricated from 316L stainless steel, allowing for thermal regulation through the circulation of a heat-transfer fluid within it;
- *(ii)* a nickel anode in the shape of a coiled grid, supplied by Neyco® (France), with a 1 mm square mesh. The geometric surface of this anode could vary based on the number of grid rotations, with surface areas of 367, 734, and 1101 cm^2 possible (illustrated in Fig. S1);
- *(iii)* an $Hg/HgO/OH^-$ reference electrode that was immersed into a Luggin capillary inserted inside the reactor;
- *(iv)* the solution volume to be treated was 0.94 L (equivalent to a S/V ratio of 39 m^{-1} for a single grid turn or 117 m^{-1} for three turns).

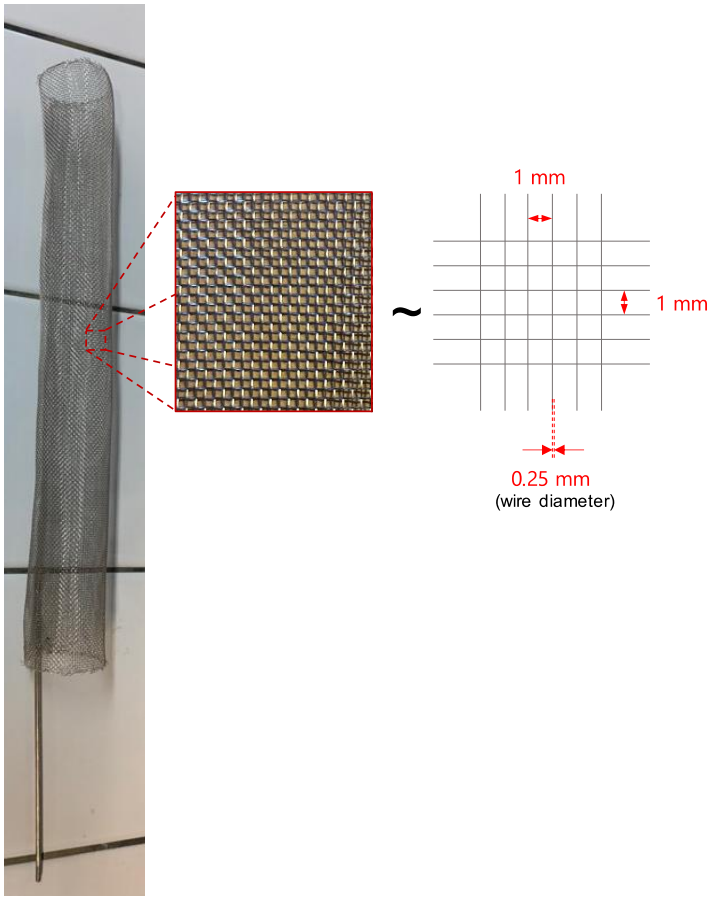

Figure S1. Nickel grid used as anode in the pilot-scale reactor.

As illustrated in Fig. S2, the reactor's environment was composed of

- *(i)* an OrigaFlex 20A potentiostat (Origalys, France);
- *(ii)* a thermoregulated liquid storage tank that also allowed for the separation of the liquid phase from the produced gaseous phase;
- *(iii)* a peristaltic pump to supply the reactor at flow rates varying from 0 to 60 $kg.L^{-1}$;
- *(iv)* a Coriolis mass flow meters to monitor the reactor feed rate, in addition to temperature and pressure sensors;
- *(v)* on the gas phase line, a thermal mass flow meter allowing to measure the mass flow rate of the gas produced, followed by a gas chromatography (GC) connected in-line to the system.

The storage tank was purged (~ 1.5 $L.h^{-1}$) with argon gas to sustain a controlled atmosphere.

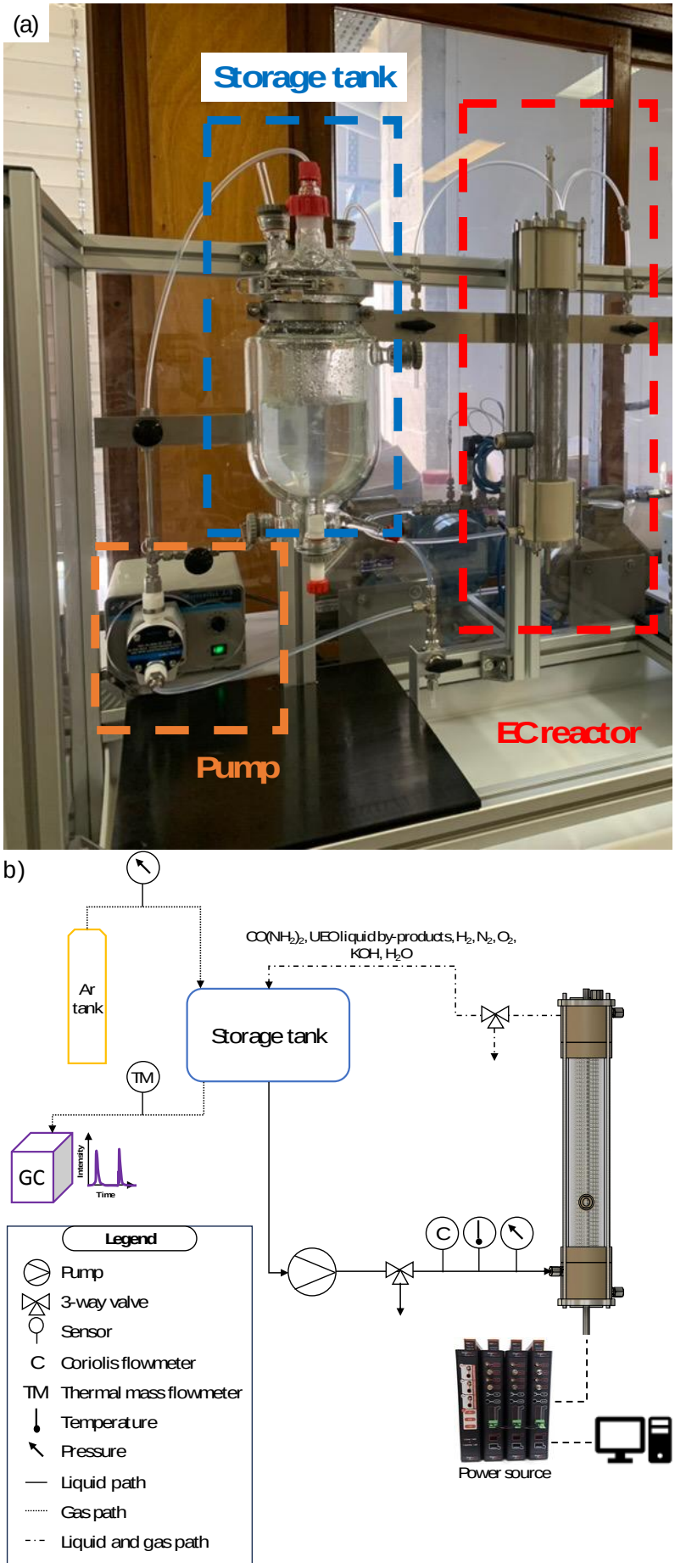

Figure S2. (a) Picture of the EC set-up at pilot-scale operating in closed loop and (b) scheme set-up.

Tab. S1 summarizes the characteristics of the pilot-scale reactor.

Table S1. Presentation of the different characteristics of the EC reactors used.

Pilot-scale (for 1 L of solution to be treated)			
Anode material	Ni mesh		
Cathode material	316L stainless steel		
S_{anode} (m^2)	3.7×10^{-2}	7.3×10^{-2}	1.1×10^{-1}
$S_{cathode}$ (m^2)	9.4×10^{-3}		
Urea/urine solution volume to treat (m^3)	9.4×10^{-4}		
S_{anode}/V ratio (m^{-1})	39	78	117
Mass flow rate Q_m ($kg.h^{-1}$)	30 – 60		
Volumetric flow rate Q_v ($L.h^{-1}$)[1]	29 – 58		
Residence time $\tau_{reactor}$ (sec)	58 – 117		
Number of passes through reactor in 1 h	31 – 62		
Reynolds number range[2]	155 – 311		

1.4 Analytical methods

The analytical methods developed to establish complete mass balances in both phases consisted in:

- *(i)* the coupling of ion chromatography (Thermo Scientific Dionex™ ICS-5000+) with mass spectroscopy analyzer Orbitrap (Thermo Scientific Q Exactive™ Focus). In our previous work [2], the method was exhaustively validated for real matrix. Thus, the operating conditions were kept unchanged in this work. This analysis enabled the measurements of ion concentrations in aliquots taken during the electrolysis (Cl^-, NO_2^-, OCN^-, CO_3^{2-} and Na^+, NH_4^+, K^+, Mg^{2+}, Ca^{2+}), as well as the ones of urea or other organic molecules present in human urine (creatine, creatinine, hippuric acid, etc.), as reported in [2];
- *(ii)* Total Organic Carbon (TOC) (SHIMADZU TOC-L) measurements [1];
- *(iii)* Inductively Coupled Plasma - Optical Emission Spectrometry (ICP-OES) (HORIBA Ultima 2) analyses [3];
- *(iv)* GC (Varian GC-450) to quantify electrolysis gas production during experiments.

The procedure was the same than the one described in a previous work [3].

1.5 Turn Over Number

[1] Density of KOH 1 $mol.L^{-1}$ solution equal to 1040 $kg.m^{-3}$

[2] The Reynolds number in the annular section (with inner and outer radius, R_1 and R_2, equal to 2 and 3 cm respectively) of the pilot-scale EC reactor was calculated as follows: $Re = \frac{2\times(R_2-R_1)\times V_d}{\nu}$ with V_d the velocity through the annular section as $V_d = \frac{Q_v}{\pi\times(R_2^2-R_1^2)}$ and μ the dynamic viscosity taken equal to 1.14 mPa.s

The Turn Over Number (TON) is reported to evaluate the catalytic answer of the UEO system [1]. Its definition is reminded in Eq. (S1).

$$TON = \frac{Q_{with\ urea}}{Q_{without\ urea}} \quad (S1)$$

It is defined as the ratio between the total charge $Q_{with\ urea}$ total associated with the entire anodic signal in the 450 – 700 mV range (as shown in Fig. S3a), which is attributed to the oxidation of Ni(II) to Ni(III) in the presence of urea, and the charge $Q_{without\ urea}$ corresponding to the complete signal of nickel oxidation without urea (as seen in Fig. S3b).

The value of TON suggests the number of times the catalytic cycle (EC') occurs between urea/NiOOH/OH^-.

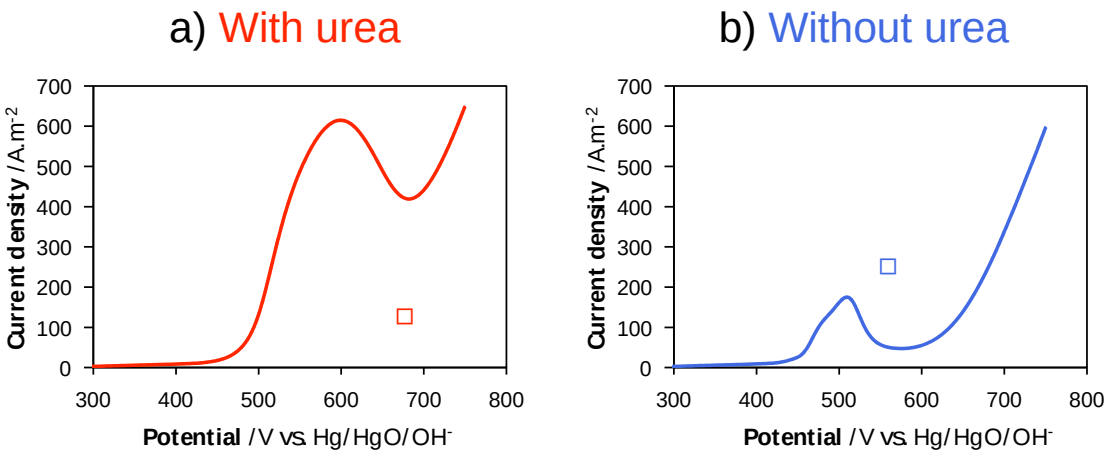

Figure S3. Linear voltammograms obtained on nickel RDE (3.14 mm^2, 1000 RPM) at 0.12 $mV.s^{-1}$ in 1 $mol.L^{-1}$ KOH a) in presence of 0.33 $mol.L^{-1}$ of urea and b) in absence of urea.

2 Linear voltammetry of main compounds in human urine in various matrices

The curves presented in this appendix were obtained in linear voltammetry (10 $mV.s^{-1}$, 1000 RPM), during different spiking of the main organic molecules and ions contained in human urine in 3 different matrices: *(i)* KOH (Fig. S4), *(ii)* urea/KOH (Fig. S5) and *(iii)* alkalinized urine (Fig. S6).

Finally, a summary illustration (Fig. S7) shows the ratio values ($\frac{I^{net}_{at\ 0.55\ V}}{I^{net}_{before\ spiking}}$) before spiking and after spiking at maximum concentration (*i.e.*, 50 $mmol.L^{-1}$).

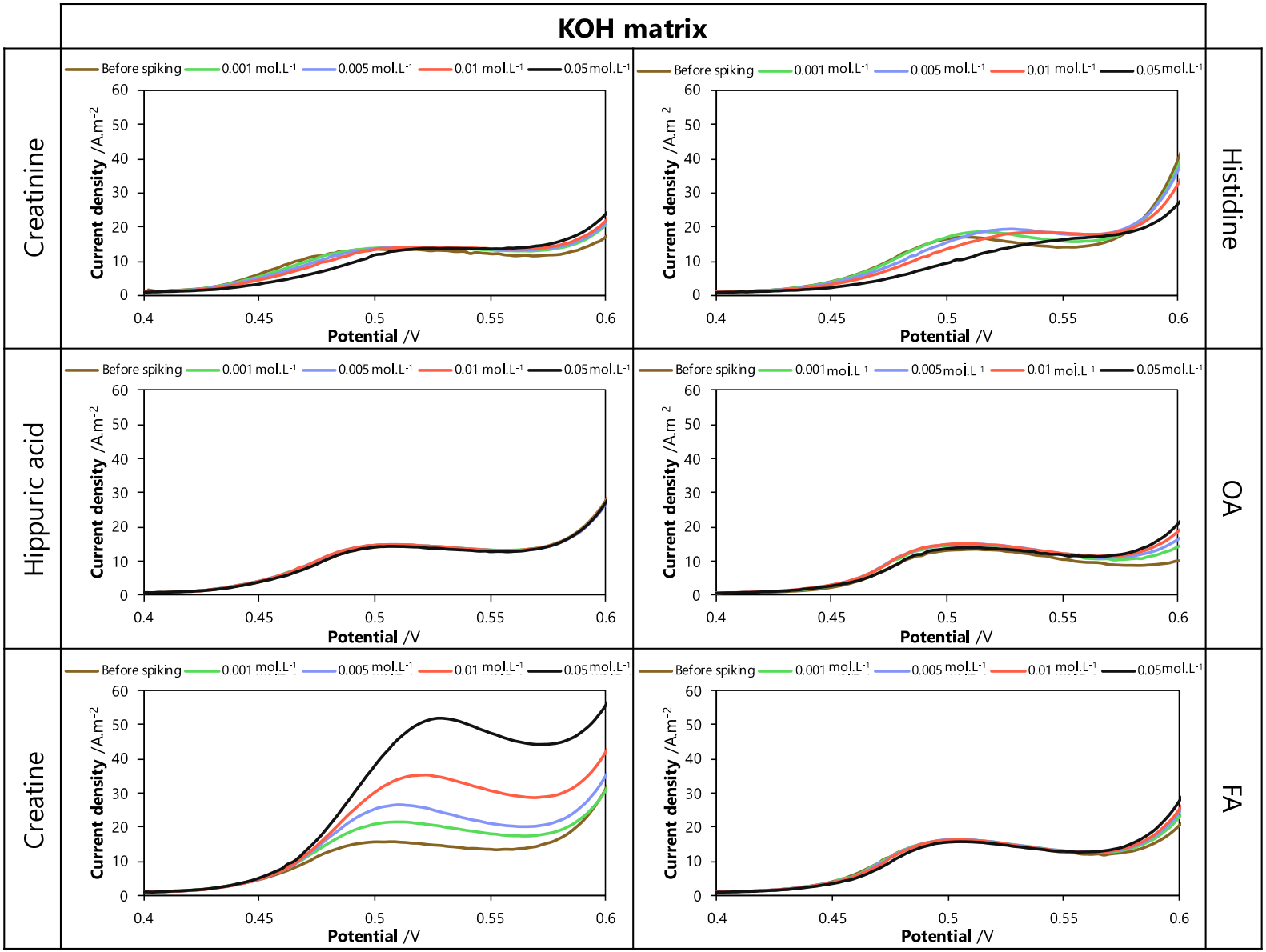

Figure S4. I-E curves obtained by spiking various compounds, mainly present in human urine, into a KOH matrix.

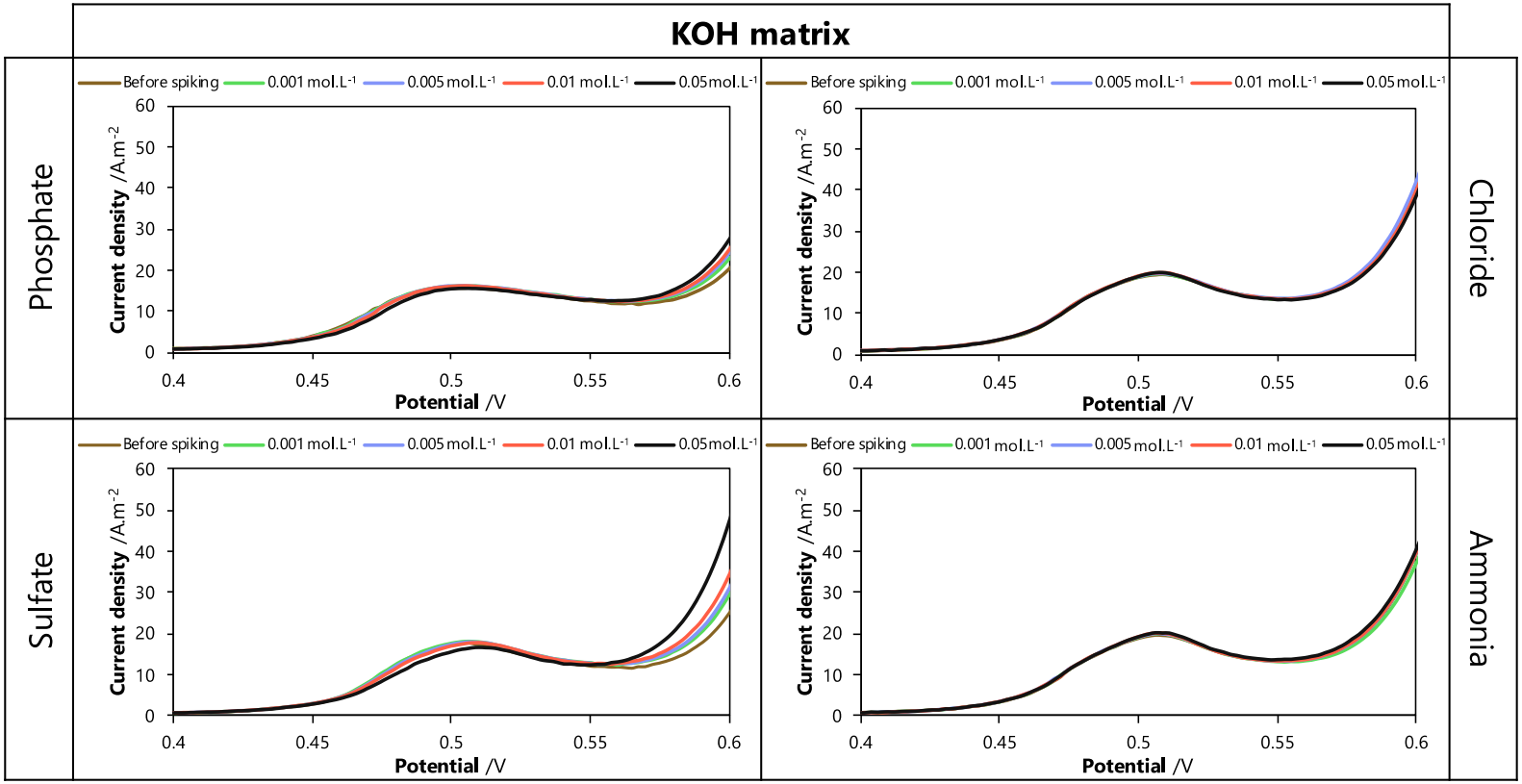

Fig. S4 (continued).

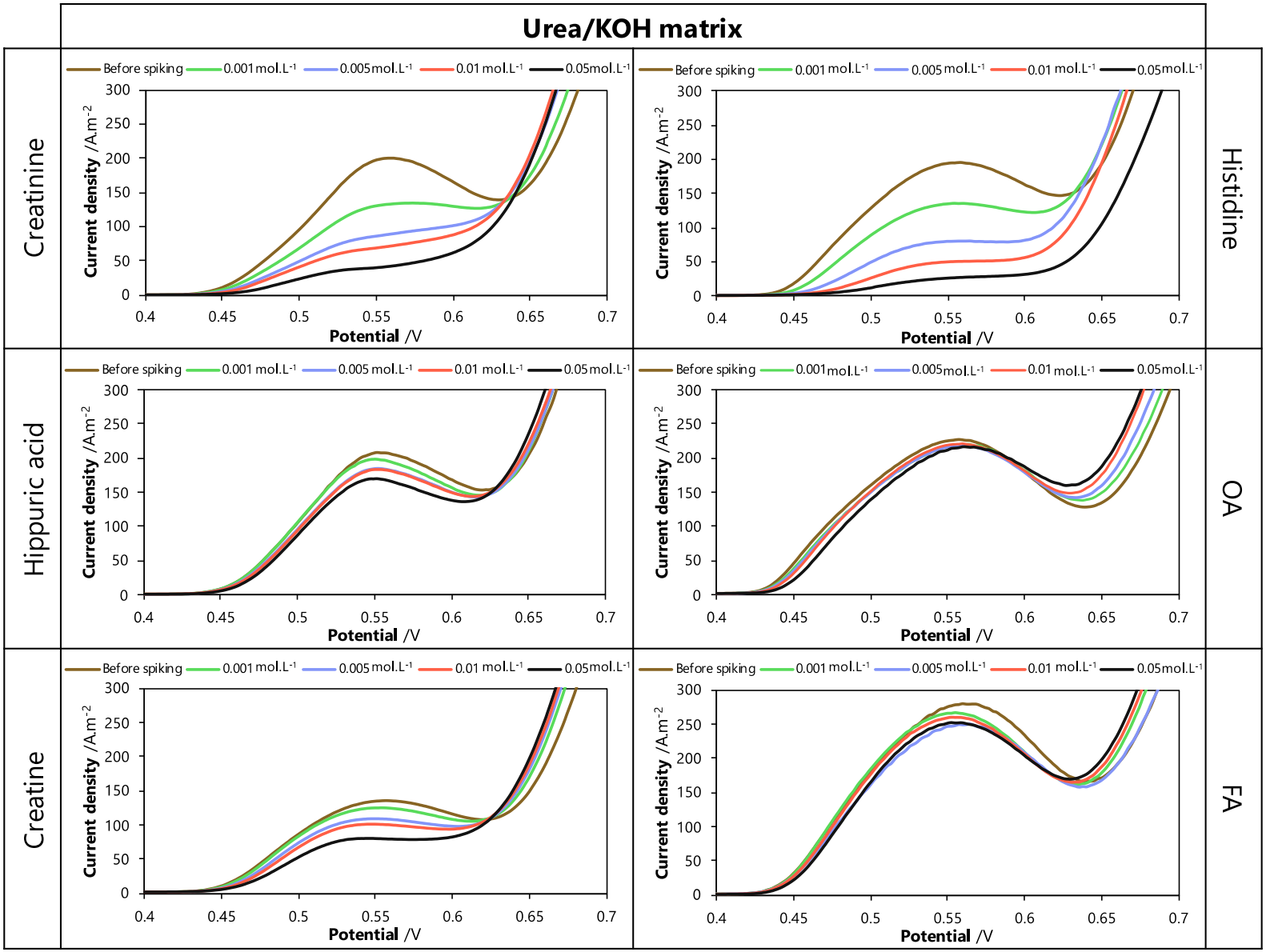

Figure S5. I-E curves obtained by spiking various compounds, mainly present in human urine, into a urea/KOH matrix.

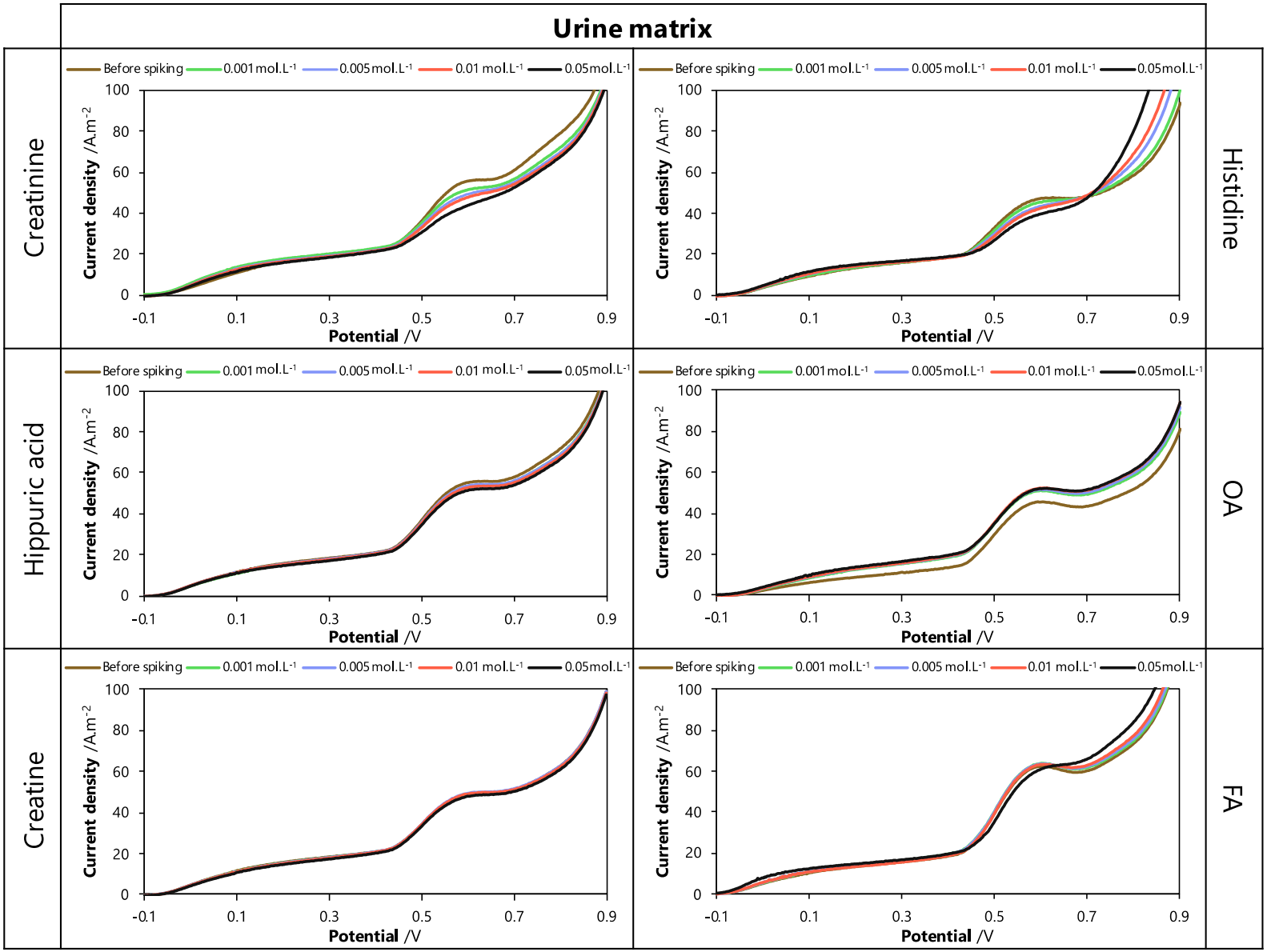

Figure S6. I-E curves obtained by spiking various compounds, mainly present in human urine, into a urine/KOH matrix.

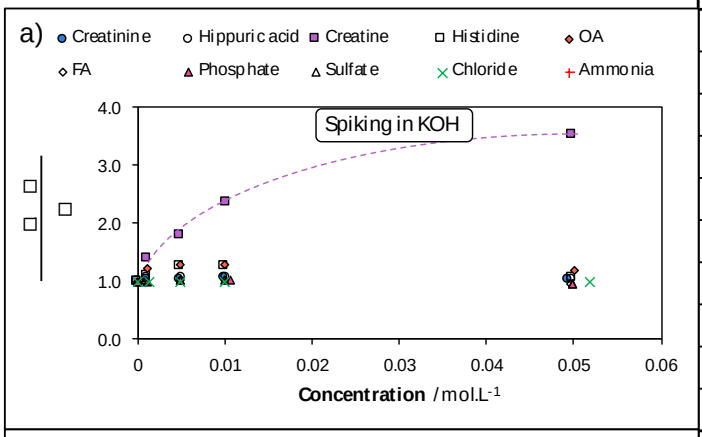

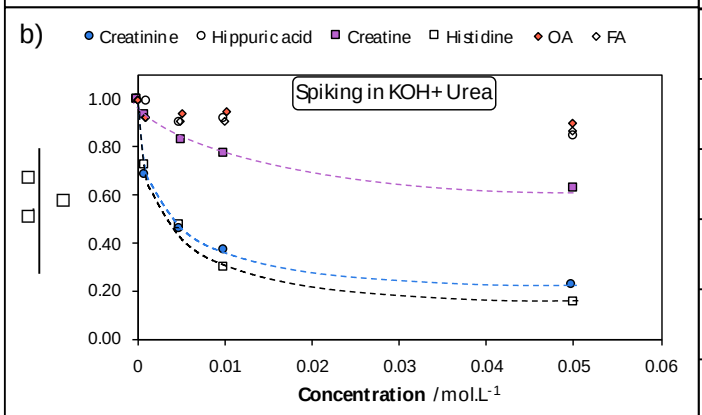

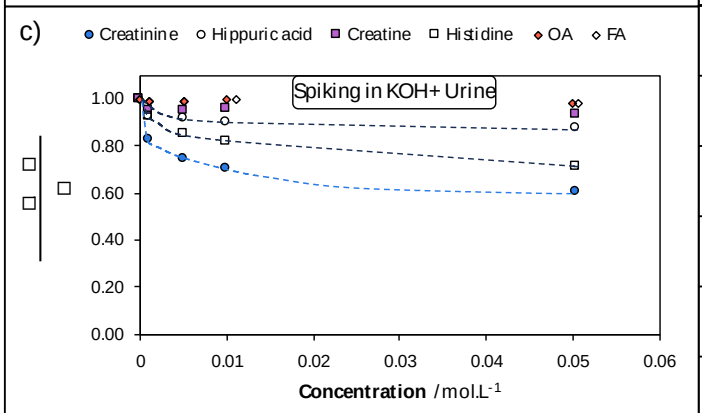

Compound	□ × (A)	□ □ × (A)
Creatinine	3.7	3.9
Hippuric acid	4.1	4.2
Creatine	4.4	15.7
Histidine	4.4	4.7
OA	3.4	4.1
FA	4.7	4.6
Phosphate	4.7	4.6
Sulfate	5.2	5.0
Chloride	5.8	5.9
Ammonia	5.9	6.0
Creatinine	60.9	13.5
Hippuric acid	61.2	51.4
Creatine	40.1	25.0
Histidine	58.7	9.0
OA	68.7	61.7
FA	83.3	72.0
Creatinine	11.5	7.0
Hippuric acid	11.1	9.7
Creatine	9.2	8.6
Histidine	9.1	6.4
OA	10.2	10.0
FA	13.9	13.6

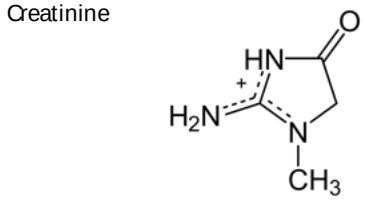

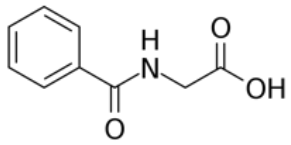

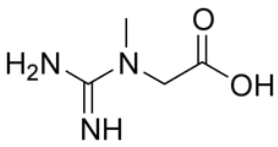

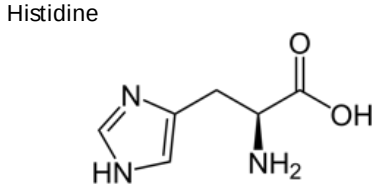

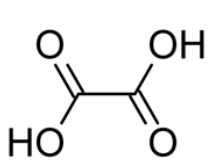

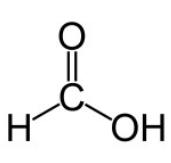

Figure S7. Summary values obtained during the spiking of various compounds in different matrices: a) KOH, b) urea/KOH and c) urine/KOH.

3 Langmuir model for histidine adsorption on nickel(III) sites

The Langmuir model assumes that the adsorbed molecules form a single mono-layer on the surface. Each site for adsorption is equivalent in terms of adsorption energy. There is no interaction between adjacent molecules.

On the basis of the adsorption reaction, one can establish Eq. (S2).

$$\Theta = \frac{\Gamma_H}{\Gamma_{H,max}} = \frac{K \times [Histidine]}{1 + K \times [Histidine]} \quad (S2)$$

where Γ_H is the number of nickel sites covered by histidine (mol.m^{-2}), $\Gamma_{H,max}$ is the maximal number of nickel sites available to the histidine adsorption (mol.m^{-2}), Θ is the coverage ratio (dimensionless, between 0 and 1), and K is the equilibrium constant of the adsorption reaction between histidine molecules and nickel sites ($K = k_{ads}/k_{des}$, dimensionless).

For this signal (0.6 to 2 V), the current, proportional to the OH^- concentration, can be expressed by Eq. (S3). In the absence of histidine (when Θ = 0), the limiting current (I°) can be deduced from Eq. (S4), without adsorption of this molecule, allowing maximum current for hydroxide ion oxidation:

with histidine: $I = n \times \mathcal{F} \times k_{OH^-} \times [OH^-] \times S \times (1 - \Theta) \times \frac{1}{1 - t_{OH^-}}$ (S3)

without histidine: $I° = n \times \mathcal{F} \times k_{OH^-} \times [OH^-] \times S \times \frac{1}{1 - t_{OH^-}}$ (S4)

$$I = I° \times (1 - \Theta) \quad (S5)$$

where I is the current (A), n is the number of exchanged electrons (1 in the case of $OH^-_{(aq)} \rightarrow 0.25\ O_{2,(g)} + 1\ e^- + 0.5\ H_2O_{(l)}$, dimensionless), k_{OH^-} is mass transfer coefficient of hydroxide ion (m.s^{-1}), S is the geometrical area of the nickel RDE (m^2), t_{OH^-} is the ion transport number of hydroxide (dimensionless).

The ion transport number of OH^- is estimated via Eq. (S6) and represents the fraction of the total current carried in an electrolyte by OH^- specie.

$$t_{OH^-} = \frac{[OH^-] \times \mathcal{D}_{OH^-}}{[OH^-] \times \mathcal{D}_{OH^-} + [K^+] \times \mathcal{D}_{K^+}} \quad (S6)$$

Assuming diffusion coefficients of 5.3 × 10^{-9} m^2.s^{-1} for hydroxide ions [4] and 1.83 × 10^{-9} m^2.s^{-1} for potassium ions [5], the number t_{OH^-} is found equal to 0.75.

The difference in the oxidation currents of hydroxide ions ($|\Delta I|$), in the presence of histidine and in its absence, can then be expressed according to Eq. (S7).

$$|\Delta I| = |I° - I| \quad \text{(S7)}$$

$$\Theta = \frac{|\Delta I|}{I°} = \frac{K \times [\text{Histidine}]}{1 + K \times [\text{Histidine}]} \quad \text{(S8)}$$

Leading to Eq. (S9):

$$\frac{1}{|\Delta I|} = \frac{1}{I°} + \frac{1}{K \times I° \times [\text{Histidine}]} \quad \text{(S9)}$$

4 Carbon balance of urea during chronoamperometric electrolysis at pilot-scale

The carbon balance during urea electrolysis at pilot-scale is shown in Fig. S8.

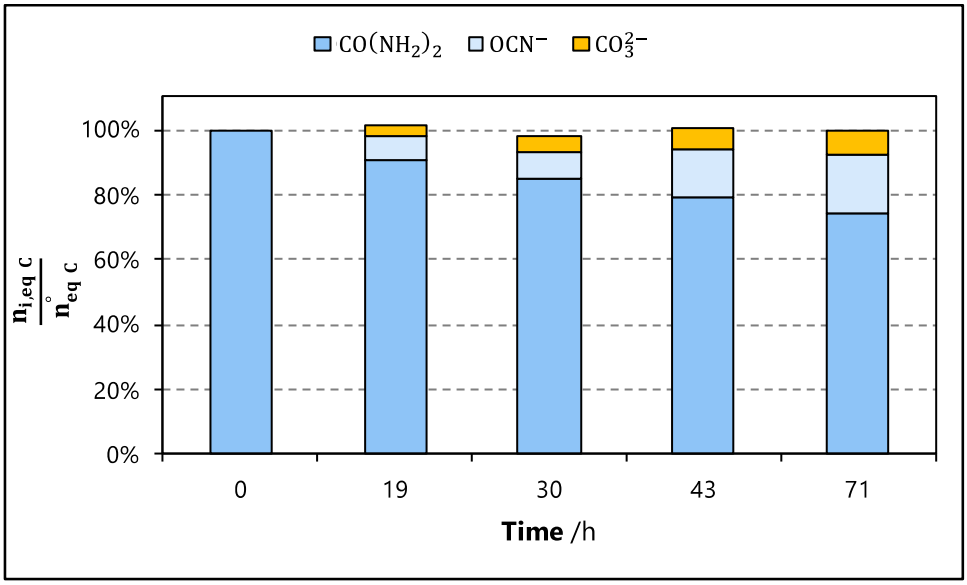

Figure S8. Typical results obtained from chronoamperometry electrolysis of a synthetic urea (0.33 mol.L^{-1}) solution in alkaline medium (1 mol.L^{-1} KOH) at pilot-scale: carbon mass balance.

5 Raw data of complete mass balances at pilot-scale when varying the anode surface

Tab. S2a shows the raw data obtained when determining the quantities of reagents and products during the chronoamperometric electrolysis of a urea solution with a Ni-surface area of 734 cm^2. Tab. S2b shows the raw data obtained when determining the quantities of reagents and products during the chronoamperometric electrolysis of a urea solution with a Ni-surface area of 1,101 cm^2.

Table S2. Raw data of reagents and products obtained at pilot-scale when varying the anode surface.

(a) Anode surface: 734 cm^2							
Time (h)	**Charge (C)**	$\mathbf{CO(NH_2)_2}$	$\mathbf{OCN^-}$	$\mathbf{CO_3^{2-}}$	$\mathbf{NO_2^-}$	$\mathbf{NH_4^+}$	$\mathbf{N_2}$
		(mol)					
0	0	0.33	0.000	0.000	0.000	0.000	0.000
19	11,600	0.30	0.020	0.010	0.010	0.030	0.001
30	15,900	0.28	0.030	0.015	0.010	0.060	0.006
43	19,600	0.26	0.050	0.023	0.020	0.070	0.008
71	25,400	0.25	0.060	0.025	0.020	0.080	0.010
(b) Anode surface: 1,101 cm^2							
Time (h)	**Charge (C)**	$\mathbf{CO(NH_2)_2}$	$\mathbf{OCN^-}$	$\mathbf{CO_3^{2-}}$	$\mathbf{NO_2^-}$	$\mathbf{NH_4^+}$	$\mathbf{N_2}$
		(mol)					
0	0	0.34	0.000	0.000	0.000	0.000	0.000
5	12,800	0.31	0.025	0.015	0.012	0.035	0.004
7	17,940	0.27	0.035	0.022	0.018	0.070	0.007
12	29,100	0.22	0.065	0.034	0.025	0.100	0.012
20	35,000	0.20	0.080	0.042	0.034	0.154	0.015

6 Raw data of complete mass balance at pilot-scale when varying the flow rate

Tab. S3a shows the raw data obtained when determining the quantities of reagents and products during the chronoamperometric electrolysis of a urea solution with a flow rate of 29 $L.h^{-1}$.
Tab. S3b shows the raw data obtained when determining the quantities of reagents and products during the chronoamperometric electrolysis of a urea solution with a flow rate of 58 $L.h^{-1}$.

Table S3. Raw data of reagents and products obtained at pilot-scale when varying the flow rate.

(a) Flow rate: 29 $L.h^{-1}$

Time (h)	Charge (C)	$CO(NH_2)_2$	OCN^-	CO_3^{2-}	NO_2^-	NH_4^+	N_2
		(mol)					
0	0	0.34	0.000	0.000	0.000	0.000	0.000
5	12,800	0.31	0.025	0.015	0.012	0.035	0.004
7	17,940	0.27	0.035	0.022	0.018	0.070	0.007
12	29,100	0.22	0.065	0.034	0.025	0.100	0.012
20	35,000	0.20	0.080	0.042	0.034	0.154	0.015

(b) Flow rate: 58 $L.h^{-1}$

Time (h)	Charge (C)	$CO(NH_2)_2$	OCN^-	CO_3^{2-}	NO_2^-	NH_4^+	N_2
		(mol)					
0	0	0.33	0.000	0.000	0.000	0.000	0.000
1	3,700	0.32	0.015	0.011	0.006	0.021	0.002
14	33,500	0.18	0.085	0.049	0.041	0.191	0.018
23	50,000	0.14	0.120	0.072	0.072	0.239	0.026

7 Illustrations observed at the end of electrolysis of human urine electrolysis at pilot-scale

During electrolysis of a real human urine solution, a coloration of the solution, formation of a foamy cloud and deposition of supernatant are observed in the reactor, as shown in Fig. S9.

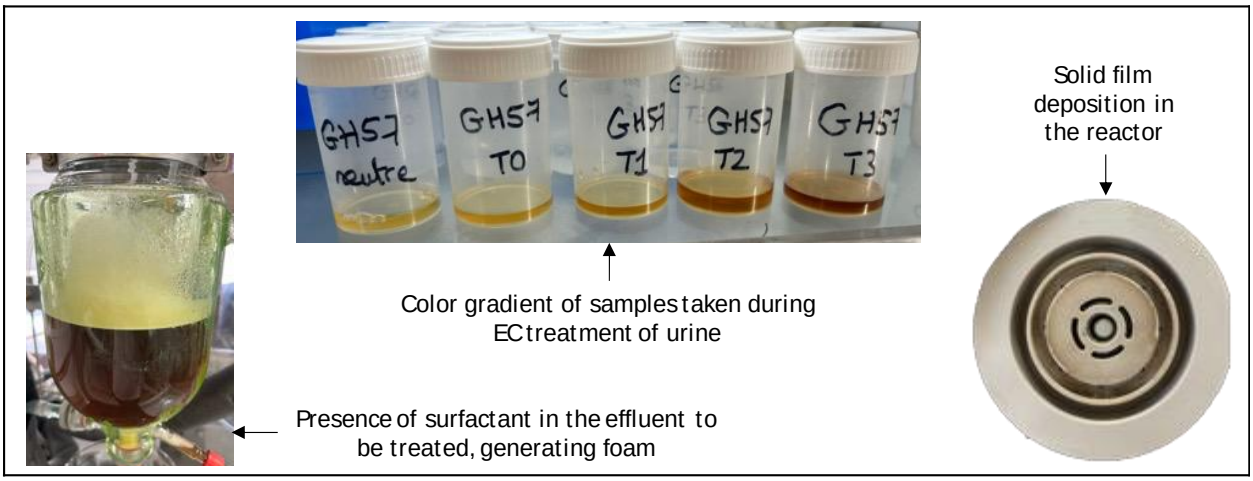

Figure S9. Illustrations related to the foam formed, the coloring of the samples and the deposit formed, all observed at the end of electrolysis.

References

[1] G. Hopsort, D. P. D. Carmo, L. Latapie, K. Loubière, K. G. Serrano, T. Tzedakis, *Electrochimica Acta*. **2023**, *442*, 141898. DOI: https://doi.org/10.1016/j.electacta.2023.141898.

[2] G. Hopsort, L. Latapie, K. Groenen Serrano, K. Loubière, T. Tzedakis, *Anal. Bioanal. Chem.* **2023**, *415* (*22*), 5337–5352. DOI: https://doi.org/10.1007/s00216-023-04808-2.

[3] G. Hopsort, L. Latapie, K. Groenen Serrano, K. Loubière, T. Tzedakis, *J. Electrochem. Soc.* **2023**, *170* (*9*), 093507. DOI: https://doi.org/10.1149/1945-7111/acf87e.

[4] E. Samson, J. Marchand, K. A. Snyder, *Mater. Struct.* **2003**, *36* (*3*), 156–165. DOI: https://doi.org/10.1007/BF02479554.

[5] M. G. He, S. Zhang, Y. Zhang, S. G. Peng, *Opt. Express*. **2015**, *23* (*9*), 10884. DOI: https://doi.org/10.1364/OE.23.010884.